J Polym Res (2017) 24: 232
https://doi.org/10.1007/s10965-017-1388-z

ORIGINAL PAPER

Fabrication of polycaprolactone/zirconia nanofiber scaffolds using electrospinning technique

V. G. Thakare[1] · P. A. Joshi[2] · R. R. Godse[2] · V. B. Bhatkar[3] · P. A. Wadegaokar[2] · S. K. Omanwar[1]

Received: 31 January 2017 / Accepted: 5 November 2017 / Published online: 28 November 2017
© Springer Science+Business Media B.V., part of Springer Nature 2017

Abstract In the present study we have investigated the effect of Zirconia (ZrO_2) nanoparticles on the fiber morphology, swelling, degradation activity and enhanced cell adhesion of the electrospun polycaprolactone (PCL) non-woven nanofiber scaffolds. The composite nanofibers scaffolds were obtained with ZrO_2 weight contents varying in the range 6% to 30%. The effect of the ZrO_2 nanoparticles concentration on the fiber morphology was investigated using a Field effect scanning electron microscopy (FE-SEM). We also investigated the degradation and swelling activities of the fabricated material. The results demonstrated better swelling with controlled degradation in comparison to the PCL scaffolds. Cell viability studies proved the non toxic nature of the nanocomposite scaffolds. Interestingly, the scaffolds with ZrO_2 nanoparticles showed enhanced fibroblast proliferation and improved bioactivity of the scaffolds. Further, this is the first report regarding the ability of a biomaterial containing ZrO_2 nanoparticles to enhance cell adhesion and proliferation.

Keywords Polycaprolactone · ZrO_2 nanoparticles · Electrospinning · Scaffold · Tissue engineering

✉ V. G. Thakare
vaishaliwatile@gmail.com

[1] Department of Physics, SGB Amravati University, Amravati (MS) 444 602, India

[2] Department of Biotechnology, SGB Amravati University, Amravati (MS) 444 602, India

[3] Department of Physics, Shri Shivaji Science College, Amravati (MS) 440012, India

Introduction

In recent year, tissue engineering offers a new approach to regenerate diseased or damaged tissue such as bone [1, 2]. The rapidly growing research in tissue engineering area thus provides a new promising approach for repair and regeneration of bone tissue [3]. Biomaterials are required in tissue engineering strategies for the fabrication of scaffolds to provide a three-dimensional (3D) biocompatible support for cell attachment, proliferation and differentiation [4, 5].Biomaterials for bone tissue engineering should combine unique biocompatibility, bioresorbability and bioactivity with excellent mechanical properties [6, 7]. Scaffolds made of such biomaterials have the potential to induce bone regeneration and are able to degrade after a certain period of implantation [4]. In comparison to other forms of scaffolds, the nanofibrous scaffolds promote cell adhesion, proliferation and differentiation more efficiently due to having high surface to volume ratio and morphological similarity to natural extracellular matrix (ECM) will allow the diffusion of nutrient, metabolites and soluble factors until the seeded cells can produce a new functional matrix and regenerate the desired tissue structures [8, 9]. A great deal of effort has been put into the design of scaffolds and the concept has evolved from inert biomaterials serving as structural support for cells in terms of tissue development [10].

However, there are several general characteristics considered the suitability of a scaffold for the use of tissue engineering [11, 12]. The very first requirement of any scaffold for tissue engineering is that the material should be biocompatible, cell must be adhere, function normally without eliciting undesirable local or systemic responses such as rejection, inflammation or immune activation, in the host. Secondly, most tissue engineering applications and tissue regeneration approaches require scaffolds that are fully biodegradable or absorbable. It is useful if the degradation rate of the scaffold

matches the rate of tissue regeneration to optimize the transfer of functions from the artificial matrices to native ECM on a time dependent basis during tissue regeneration. Faster rates of degradation of the scaffold may lead to a loss of tissue integrity and function, while a degradation rate that is too slow can result in barriers to transport or mechanical mismatches such as stress shielding, resulting in long term failure of the system. In addition, the scaffold architecture used for tissue engineering is also important. Scaffolds should have an interconnected pore structure and high porosity to ensure the cell penetration and diffusion of nutrient to cell within construct and to EMC formed by these cells. Moreover, this structure is desirable for locally sequestering and delivering bioactive molecules, and providing space for tissue ingrowth. Scaffolds should also be mechanically matched to the target tissue. It should be reproducible, cost effective and scalable. In order to realize the active role of artificial scaffolds in regulating the behavior of cells, the interface between the biomaterial and the cells must be examined.There are also research efforts in producing scaffolds from other oxide ceramics, notably alumina, titania and zirconia. Although these are not biodegradable ceramics, they find application in ex vivo approaches or in bioreactors. Bioceramic scaffolds exhibiting highly porous structures are being fabricated (with different degrees of success) by a variety of techniques, as reviewed elsewhere [13].

Various technologies have been developed to fabricate three-dimensional (3D) scaffolds [8], such as drawing, Template synthesis, temperature induced phase separation, self assembly and electrospinning [14] in which electrospinning has been widely use for the fabrication of nanofibers scaffolds. It is simple, elegant and versatile technology for producing ultrathin non-woven fibers with a diameter ranging from nanometers to microns [9, 10]. Among different available scaffolds, those recently developed with nanofibrous structures seem to be promising substrates for tissue engineering applications due to their high structural similarity to native extracellular matrix, continuous high surface to volume ratio, high interconnected porosity and variable pore size distribution [15, 16]. A variety of materials including polymers, ceramics and their composites can be electrospun into fibrous scaffolds [16]. However, Polycaprolactone (PCL) is widely used in tissue engineering to construct the scaffold. It has some advantages over other polymer and is more stable in ambient conditions, less expensive and readily available in large quantities. Yoshimoto et al. reported that electrospun PCL scaffolds provide an environment that supports mineralized tissue formation and may be a suitable candidate for the treatment of bone defects. The shapeability of electrospun PCL scaffolds may also prove useful in clinical applications and scaffolds produced by using PCL matched the design very well, had compressive strength and modulus value within the range of trabecular bone and supported the in-growth of bone in an in vivo model [17]. PCL is a slow-biodegrading polymer has been used for potential applications in bone, cartilage repair [18]. This application of PCL might be limited in the field of drug delivery or resorbable sutures due to its slow degradation and resorption kinetic, but this slow degradation could be beneficial for bone tissue engineering. It gives time for osteoblasts to build up the bony tissue and in parallel to the bone regeneration the implant will slowly degrade [19].

In recent year,Ceramics are increasingly used for biomedical application [20] and previous studies have shown better cell growth and enhanced cellular behavior on nanophase ceramics that is titania, Zirconia and alumina as compared to conventional (μm size) ceramics [21, 22], in which zirconia is considered to be one of the most used materials after titanium, especially in dentistry [23]. Zirconia was introduced 20 years ago to solve the problem of aluminum brittleness and the consequent failure of orthopaedic implants [24]. It has advantages over other ceramics because of its high mechanical strength and fracture toughness. Zirconia also finds other clinical applications such as: arthroplasty [25], dental crowns [26] hip and knee prostheses, hip joint heads, temporary supports, tibial plates [27]. At tissue level, Zirconia was found to be as biocompatible as titanium. Cultured osteoblasts proliferate and differentiate on zirconia without producing any adverse reaction [28]. In vivo studies indicate that ZrO_2 implants exhibit excellent osteointegration and zirconium-related materials, such as zirconia ceramics and coatings, have previously been used as bone implant materials [29]. Hence, zirconia is considered a bio-inert ceramic because when implanted it only shows a morphological fixation with the surrounding tissues without producing any chemical or biological bonding [30, 31].

Therefore, we are focusing on the fabrication of PCL/ZrO_2 nanofiber composites scaffolds using electrospining technique. Structure and morphology of PCL/ZrO_2 scaffolds were investigated. Biological evaluation of these hybrid materials was carried out by cytotoxicity investigation using 3T3 mouse fibroblast cell line. The ability of the prepared scaffolds to attach the cell and proliferation was investigated. Swelling and in vitro degradation of prepared scaffolds was also evaluated.

Materials and method

Materials

The polycaprolactone (MW = 80,000), MTT [3-(4,5-dimethyl-2-thiazolyl)-2,5-diphenyl-2H-tetrazolium bromide], Dimethyl Sulphoxide and DAPI (2-(4-amidinophenyl)-1H -indole-6-carboxamidine) used in this study were purchased from Sigma Aldrich, St. Luis, USA. Dulbecco Modified

Eagle's Medium (DMEM) and fetal bovine serum (FBS) were procured from Gibco, USA and Himedia, Mumbai, India respectively. Acetone and ethanol were obtained from Merck, Mumbai, India. All the reagents used in this study were of analytical grade quality.

Methods

Synthesis of zirconia (ZrO_2) nanoparticles

ZrO_2 nanomaterial was prepared using well established modified solution combustion technique [32, 33]. During the reaction the stoichiometric amounts of ingredients including all precursor Zirconium nitrate (3.39 g), Ammonium nitrate (6.4 g) (oxidizer) and Glycine (3 g) (fuel), calculated on the basis of molar ratio and were thoroughly mixed in the agate mortar by adding little amount of double distilled water resulting in an aqueous homogeneous solution. Table 1 shows the balanced molar ratios of precursors used in the synthesis and corresponding chemical reactions. The solution was then transferred into a china basin. The china basin was then kept into preheated muffle furnace maintained at 450 °C. The solution boils to foams and ignites to burn with the flame and a voluminous foamy powder was obtained. The entire combustion was over in 5 min. Following the combustion the resulting fine powder was annealed in open air at 900 °C for 2 h and allowed to cool down at room temperature.

Electrospinning of PCL/ZrO_2 nanofibers scaffolds

The polymer solution of PCL at the concentration of 16% (*w/v*) was prepared by dissolving the polymer into an organic solvent mixture of acetone/ethanol (7/3 *v*/v). Pre-determined amount of the ZrO_2 nanoparticle powders were added into 10 ml mixture of acetone/ethanol (7/3 v/v). This mixture was sonicated for 20 min to disperse the zirconia nanoparticles. Then, above powder was added into polymer solution and stirred at 40 °C overnight. The mixture was further magnetically stirred for 15 min, followed by sonication for another 15 min to obtain the well-mixed PCL/ZrO_2 suspension. A ZrO_2 nanoparticle powder was varying 6 wt%, 12 wt%, 20 wt%, 25 wt% and 30 wt% with PCL concentration and made a separate PCL/ZrO_2 suspension. The PCL/ZrO_2 nanofibers composite scaffold was prepared by electrospinning technique using above mixture suspension.

Briefly, the as-prepared suspension was added into a plastic syringe equipped with a needle with an inner diameter of 1.2 mm. The syringe was then mounted onto a syringe pump in which the needle was connected to a high voltage power supply. Under 20 kV voltages, the fluid jet was injected out at a rate of 150 μl/h and the resultant nanofibers were collected on an aluminum foil which was put at 17 cm distance down from the needle. After electrospinning for 2 h at room temperature, the PCL/ZrO_2 nanofibers scaffold was obtained. Pure PCL nanofibers scaffold were also prepared as the control. The PCL and PCL/ZrO_2nanofibers scaffolds were dipped in double distilled water to remove the residual solvent for 24 h. Then, these scaffolds dried at room temperature and kept in UV-Chamber for 2 days. Figure 1 shows the experimental setup of electrospinning technique.

Cell viability studies

The viability of cells seeded on the scaffolds was determined using MTT assay. MTT assay measures the reduction of the tetrazolium component MTT by viable cells. Therefore, the level of the reduction of MTT into formazan can reflect the level of cell metabolism. 3T3 mouse fibroblast cells were seeded in 96-multiwell plates at a density of 1.0×10^5 cells/well. After 24 h of incubation, cells were treated with 200 μl culture medium solutions containing PCL and PCL/30wt%ZrO_2 scaffolds construct. Scaffolds cut into cube having dimension 1 mm*1 mm*1 mm. After 48 h of incubation, 150 μl MTT (1 mg/ml in PBS) was added and again kept for 1 h at 37 °C in a 5% CO_2 humidified atmosphere. The MTT solution was then removed and 100 μl of Dimethyl Sulphoxide (DMSO) was added to dissolve the formazan crystals. Finally, the absorbance at 570 nm was measured using the plate reader (Robonik). All data were averaged from three parallel experiments.

Cell adhesion and proliferation

Cell adhesion and proliferation studies were evaluated using 3T3 mouse fibroblast cell line. 3T3 mouse fibroblast cells were cultured in Dulbecco Modified Eagle's Medium containing 10% fetal bovine serum and 1% antibiotics and antimycotic solution in CO_2 incubator (37 °C, 5% CO_2). DMEM was replaced every two days. When 3T3 mouse fibroblast cells reached 80% confluence, they were trypsinized and counted using a hemocytometer. Cells were seeded drop wise onto the nanofiber scaffolds (1×10^5 cells/100 μl of medium/scaffold), which fully absorbed the media in 6-well plates, allowing cells to distribute throughout the scaffolds.

Table 1 The balanced molar ratio of precursors used in the synthesis and corresponding chemical reactions

Product	Corresponding reaction with balanced molar ratios of precursors
ZrO_2	$Zr(NO_3)_4 + 4C_2H_5NO_2 + 8NH_4NO_3 \rightarrow ZrO_2 +$ Gaseous products

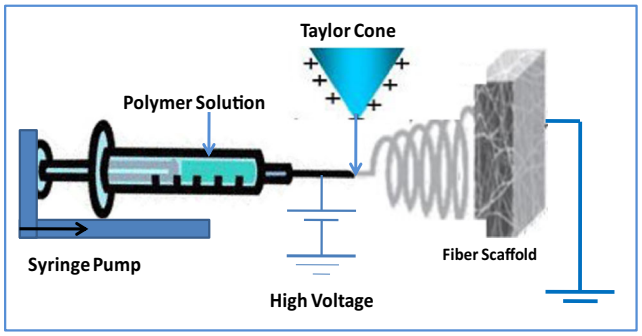

Fig. 1 Experimental setup of electrospining technique

Subsequently the cell seeded scaffolds were incubated at 37 °C in a humidified CO_2 incubator under standard culturing conditions for 1 to 7 days in order to allow the cells to adhere onto the scaffolds.

Morphology studies of nanofibers scaffold

Cell morphological studies of nanofiber scaffold were investigated using DAPI stain which bound to DNA. For DAPI staining, medium was removed from 6 well plates. The scaffold was washed three times with PBS^+ (Phosphate Buffer Saline), followed by fixing them with 3.7% Formaldehyde for 30 min. The formaldehyde was removed and washed the scaffold three times for 5 min each in PBS^+. The scaffolds were permeabilized by immersion in 0.2% Triton X-100 for 5 min and washed three times for 5 min each in PBS^+ followed by the incubation for 1–5 min at room temperature in DAPI solution (dilute 1:5000 in PBS^+). Again the scaffolds were washed three times in PBS^+.

FE-SEM morphological study of the scaffold

Morphology of cells on the nanofiber PCL and PCL30wt%ZrO_2scaffolds were evaluated for 5 and 7 days after seeding. For FE-SEM analysis, the scaffolds were taken out from the culture plate and rinsed gently with PBS, followed by fixing them with 4% Formaldehyde solution for 30 min. They were dehydrated in graded ethanol solution (30–100%) for 10 min each. Finally, they were air dried at room temperature for overnight. Dry cellular constructs were coated with gold sputter and observed under the FE-SEM.

Swelling studies

The Swelling studied of PCL and PCL/30wt%ZrO_2nanofiber scaffold were performed in PBS at pH 7.4 at 37 °C. Dryweight of scaffolds was noted (Wd). Scaffolds were place in PBS solution for 7 days. The scaffolds were removed each day to remove absorbed water on the surface and wet weight was recorded (Ww). The ratio of swelling was determined using the formula.

$$Swelling \quad ratio = \frac{Ww - Wd}{Wd}$$

In vitro degradation studies

The degradation of PCL and PCL/30wt%ZrO_2nanofiber scaffolds were studied in phosphate buffered saline solution. The pH of solution was 7.4 at 37 °C. The scaffolds were immersed in PBS and incubated for 5 weeks. After each week the scaffolds were washed in deionised water and dried. Initial weight was noted as Wo and dry weight as Wd. The degradation of scaffold was calculated by using the formula.

$$\text{Degradation}\,(\%) = \frac{Wo - Wd}{Wo} X 100$$

Characterizations

The structural morphology of the composite scaffolds was examined using Field Effect Scanning Electron Microscopy (FESEM). Nanofiber scaffold samples were prepared by taking a thin section of the nanofiber scaffold. The section was then gold sputter coated in and examined using scanning electron microscope (HITACHI S-4800). Powder X-ray Diffraction analysis of sintered samples was carried out in order to study the structural properties of Zirconia using a rigaku diffractometer (XRD, miniflex rigaku), and then analyzed, using Ni-filtered CuKα radiation ($\lambda = 0.1542$ nm) in the step scanning mode, with tube voltage of 40 kV and tube current of 40 mA. The XRD patterns were recorded in the 2θ range of 20 to 70°, with a step size of 0.02° and step duration of 1 s. FTIR study was done using Shimadzu Fourier Transform Infrared Spectrophotometer. The morphology of the cells over the scaffold was studied under Inverted light microscope (Magnus, Invitrogen) and Fluorescence Microscopy (FLoid Cell Imaging system, Life Technologies, Themofisher) using DAPI stain ($\lambda ex \approx 395$ nm, $\lambda em \approx 461$ nm).

Results and discussions

Characterization of ZrO_2 nanoparticles

It is well known that nano structured materials exhibited unique physiochemical properties that are unseen in conventional bulk materials. Nano-ZrO_2 exhibits much better structural and biological properties as compared to normal ZrO_2 powder, due to the small particle diameter which will result in

better sintering ability [34, 35]. Nano- ZrO_2 particles can be prepared by a variety of approaches, for example, wet chemical/precipitation, Sol-gel [36, 37] methods. In the present work combustion synthesis was employed. FE-SEM images of nano $ZrO_2$are as shown in Fig. 2a. It shows that homogenous distribution of particles with spherical morphology. The Fig. 2b shows the particles of average diameter 33.375 nm. The formation and composition of crystalline of ZrO_2 nanoparticles are confirmed from Energy Dispersive X-ray (EDX) analysis, Fig. 2d revealed that the Zr and O are the only elements in the sample with high purity and no other impurity.

X-ray Diffraction pattern (XRD) also revealed the pure Zirconia phase with high crystallinity (Fig. 2c). It is well match to ICCD data file number 01–078-1807. The particle size of ZrO_2 materials was calculated using Scherrer equation [38, 39].

$$D = \frac{K}{\beta cos\Theta}$$

Where λ is the wavelength CuKα radiation, β is the full width at the half maximum of ZrO_2 (211), $2\Theta = 31.373^0$ reflections which have the highest intensity among ZrO_2 peaks and Θ is the diffraction angle. The mean crystalline size was found that 23 nm. Particle size is one of the crucial factors influencing the integrity of the scaffolds [40].

Morphology of the nanofibers scaffolds

Analyzing the effect of ZrO_2 nanoparticles on the fiber morphology and structure revealed the spider web structure of the scaffolds. It may be observed from the micrographs that the resulting PCL and PCL/ZrO_2nanocomposite fiber scaffolds are almost uniform in fiber morphology and are highly porous. The effect of ZrO_2 nanoparticles of various concentrations, a lower range of 6 wt%, and a higher range of 30 wt% does not shows changed in fiber morphology. As can be seen from Fig. 3 uniform and highly smooth nanofibers were formed without the occurrence of bead defects for all materials. Both the control PCL and PCL/ZrO_2 electrospun scaffolds showed an interconnected and highly porous structure which was composed of continuous nonwoven nanofibers.

FTIR analysis

Figure 4 shows the FT-IR spectra of polycaprolactone and PCL/ZrO_2 nanofibers scaffold. FT-IR analysis of PCL/ZrO_2 nanofibers scaffold revealed the incorporation of ZrO_2 into the PCL matrix. FT-IR spectrum of neat PCL shows an intense peak at 1728 cm^{-1}, which is due to the presence of the ester carbonyl group that corresponds to the -CO (stretching) in the PCL polymer. The peaks at 2864 and 2941 cm^{-1} are related to the C–H bond of saturated carbons. The PCL/ZrO_2 and polycaprolactone presented the same spectra in the wave number range of 700–4000 cm^{-1}, while the peak located at 500–700 cm^{-1} is attributed to the stretching of the Zr-O bond [41–43]. It is clearly seen in Fig. 4b.It means that Zirconia is well incorporate in PCL polymer matrix. Figure 4b showed additional Peak at 1629 cm^{-1} belongs to the bending mode of OH group while the sharp peak at 3570 cm^{-1} denotes the OH stretching vibrations. The absorptions at, 3535 cm^{-1}, 3508 cm^{-1} correspond to the vibration of stretching and deformation of the O-H bond due to the absorption of water and coordination with water [44].

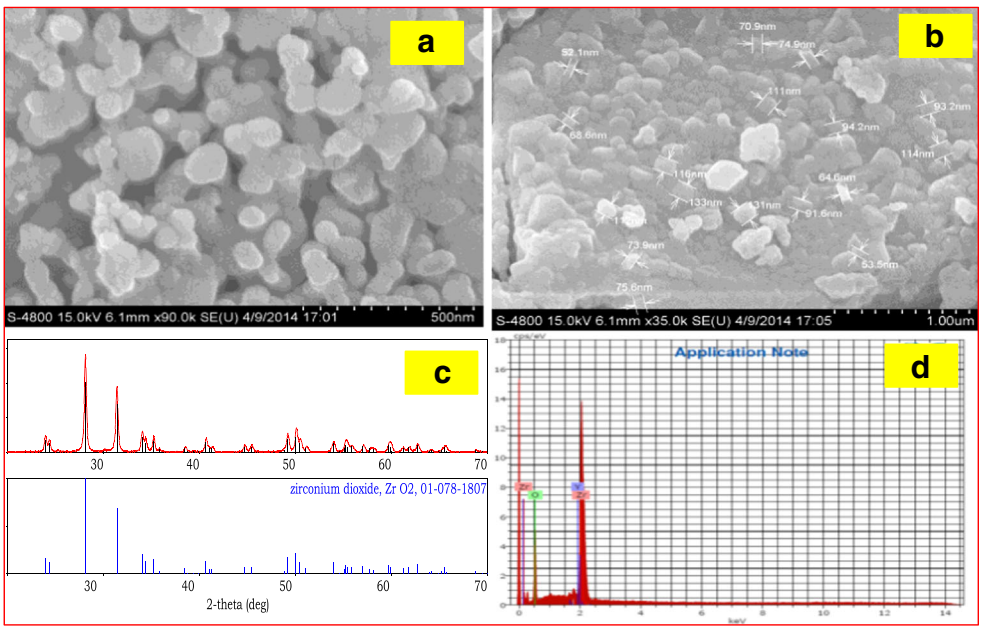

Fig. 2 **a-b** FE-SEM images of the nano ZrO_2 particles at different magnification (**c-d**) are XRD patterns and energy-dispersive X-ray spectrum (EDX) of the of the nano ZrO_2, respectively

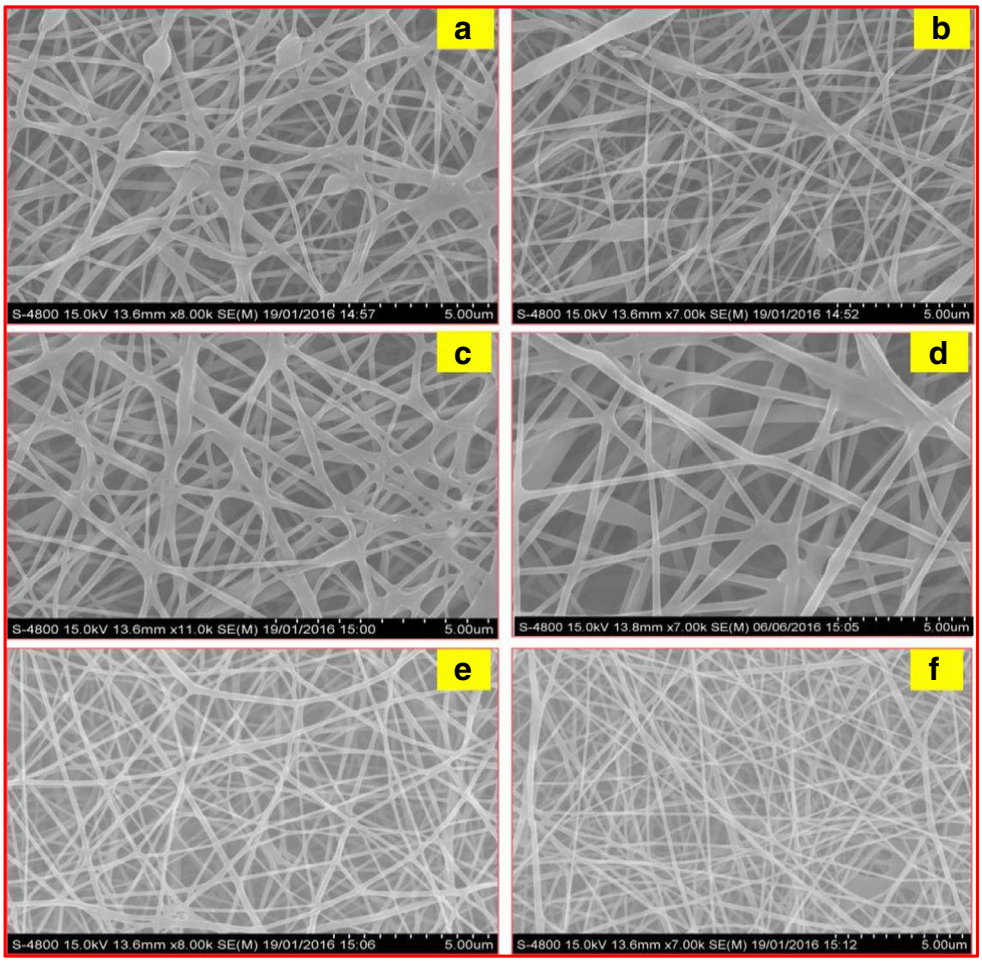

Fig. 3 FE-SEM images to show surface morphology of (**a**) PCL (**b**) PCL/6wt%ZrO_2 (**c**) PCL/12wt%ZrO_2 (**d**) PCL/20wt%ZrO_2 (**e**) PCL/25wt%ZrO_2 (**f**) PCL/30wt%ZrO_2 nanofibers scaffolds

Cytocompatibility studies

Mouse fibroblast cells (3T3) were incubated for 48 h in standard growth medium at 37 °C in 5% $CO_2$and 95% air environment in the presence of PCL and PCL/30wt%ZrO_2 scaffolds. The result from this study revealed that cell viability was 71%, 72% and 73% for control (00 μ), PCL and PCL/ZrO_2 scaffolds as shown in Fig. 5.The results suggest that there are no significant ($p \geq 0.005$) effect in the PCL/ZrO_2 scaffolds in comparison to the control PCL scaffolds. This study proved the nontoxic nature of composite scaffolds against 3T3 mouse fibroblast cells. Hence it suggests that cell viability is not affected by addition of nano ZrO_2. The cytocompatibility of ZrO_2 has already been proved earlier [21].

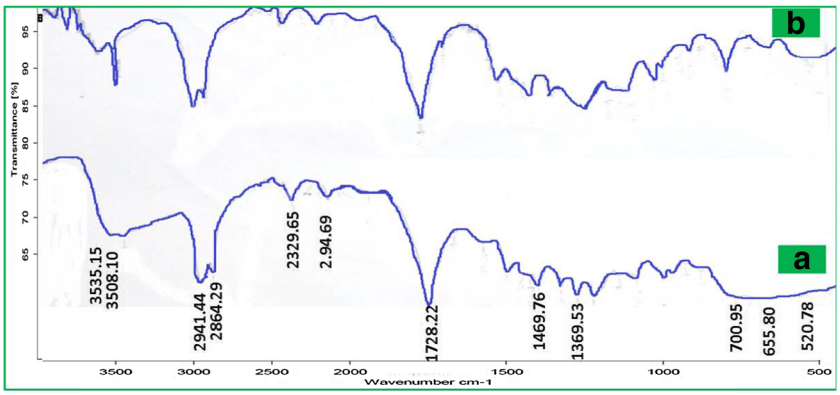

Fig. 4 FTIR spectra of (**a**) PCL (**b**) PCL/30wt%ZrO_2

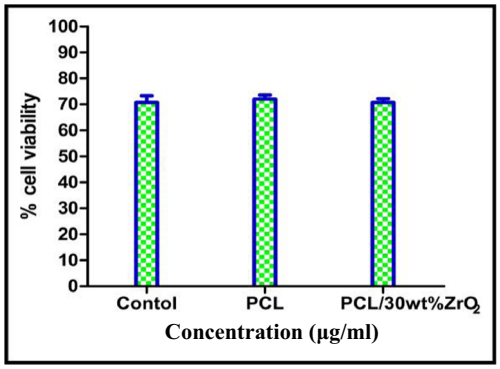

Fig. 5 Effect of PCL and PCL/30wt%ZrO_2 scaffolds on 3T3 mouse fibroblast cells. Data is represented as Mean ± SEM ($n = 3$)

Cell adhesion and proliferation studies of the nanofibers scaffolds

The PCL/30wt%ZrO_2 nanofibers scaffold was selected for further study and PCL scaffold was used as a control. Inverted Microscope images were used to study the attachment, morphology and spreading of cells on the PCL/30wt%ZrO_2nanofibers scaffolds. Inverted Microscope images of cells incubated for 2, 3, 5 and 7 days on the scaffolds showed the cells attachment and spreading on the scaffolds (Fig. 6). However, there was a difference in morphology and spreading in a material dependent manner. After 3 days of incubation cells (3T3) on the control scaffolds remained in less number and localized, while cells were found to be migrated towards the nanofiber scaffolds with a well spread morphology and higher cell density. After the 7 day period of incubation, cell attachment studies showed that the nanofiber scaffold has increased cell attachment as compared to control scaffolds. The higher attachment on nanofiber scaffolds may be due to the increase in surface area. It is known that surface topology could play a role in cell attachment on implants [45]. An increase in surface area allows maximum area for cell attachment and nano surfaces have larger surface area to volume ratio [46]. The new composite nanofibers could provide

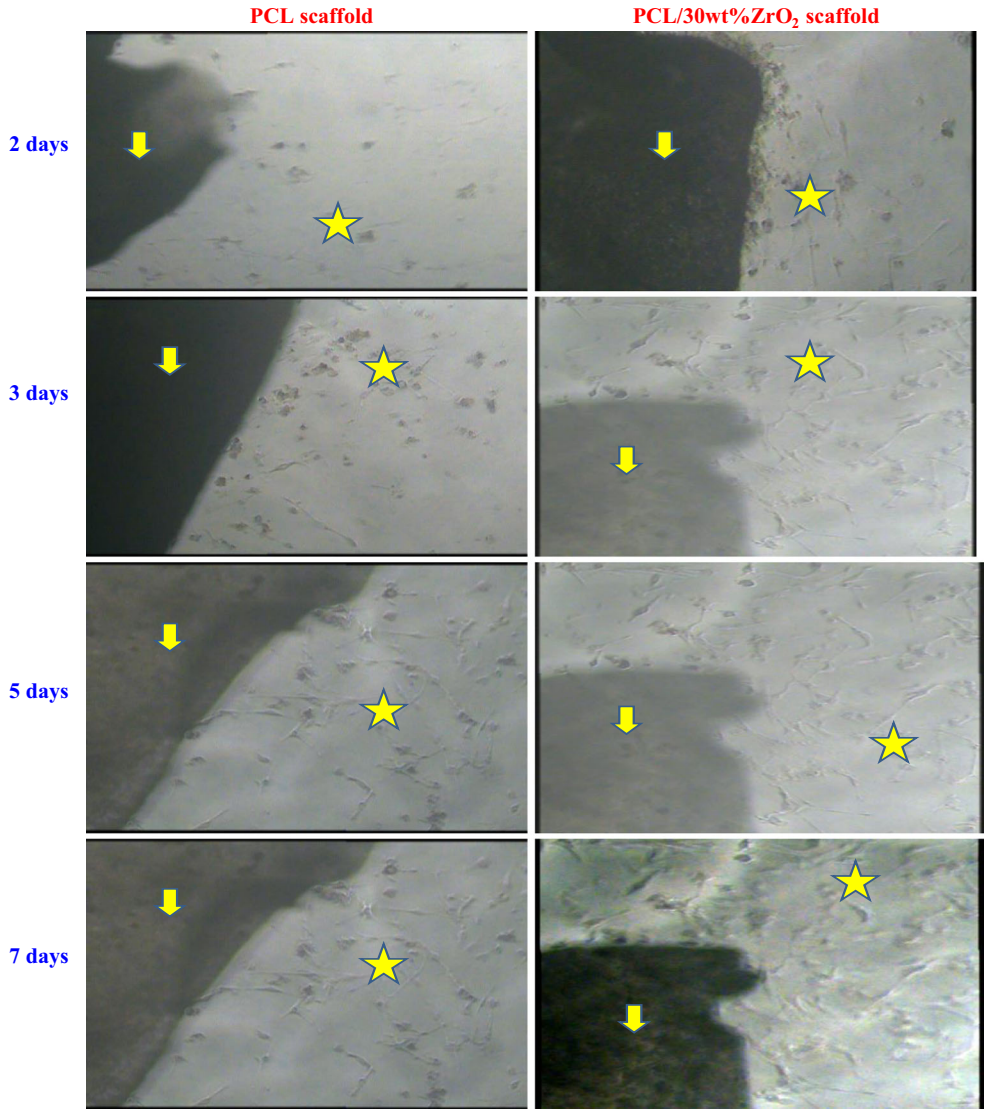

Fig. 6 Optical microscopy images of a culture of mouse fibroblasts 3T3 cells in contact with the PCL and PCL/30wt%ZrO_2 nanofibers scaffold (stars indicate fibroblast cells and Arrows indicate scaffolds surface)

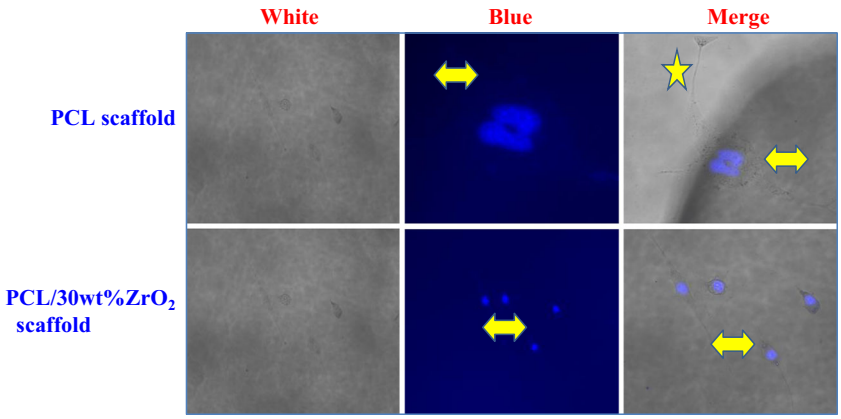

Fig. 7 Fluorescence microscopy images of a culture of mouse fibroblasts 3T3 cells in contact with the PCL and PCL/30wt%ZrO_2 nanofibers scaffold for 3 days (stars indicate fibroblast cells and left-right arrows indicate growth of fibroblast cells on scaffolds surface)

better hydrophilicity (wettability) and improved biological properties. Biologically, the incorporation of ceramic into the synthetic components could promote cell-surface recognition and also promote or control many aspects of cell physiology such as adhesion, spreading, activation, migration, proliferation and differentiation. Due to the size of the nanofibers, such effects are being augmented or made more effective because of the high surface area for cells to access [47].

Cell morphology and proliferation studies of the nanofibers scaffolds

DAPI staining was used to evaluate cell attachment and proliferation by staining of cell nuclei. The 3T3 mouse fibroblast cells were incubated on the scaffolds and examined under fluorescence microscope for 3, 5 and 7 days (Figs. 7, 8, and 9). Fluorescence microscope images showed that cells attached to the scaffolds with spindle fibroblast-like morphology, a characteristic feature of 3T3 mouse fibroblast cells. The ideal scaffold should have ability to support the attachment of cells on its surface [48, 49].

After 3 days of cell seeding the cells were attached to the scaffold and the morphology of cell was clearly observed on the surface of scaffold (Fig. 7). The scaffolds substrate supports the cell attachment and proliferation after 5 days (Fig. 8). After seeding the same number of cells on scaffolds for 7 days (Fig. 9), fluorescence micrographs showed that the majority of the cells that had been grown on PCL and PCL/30wt%ZrO_2 scaffolds showed the spindle morphology.

Comparatively, between the PCL nanofibers and the PCL/30wt%ZrO_2 substrates, the number of cells that were attached on the PCL/30wt%ZrO_2 nanofibrous substrates was more than that of the cells attached on PCL scaffold (Figs. 7 and 8). Comparing PCL and PCL/30wt%ZrO_2 scaffolds, the notable increase in the number of attached cells was observed on the PCL/30wt%ZrO_2 scaffold after 7 day cell culturing (Fig. 9). The blue and merge images clearly indicated that cells were attached on the surface of scaffolds and around the surface of scaffolds and increases in number of cells after 7 days.

Morphology and surface chemistry of nanofibers scaffolds used in tissue engineering and regenerative medicine have an important impact on cell behaviors such as adhesion, proliferation, differentiation and cell-matrix interaction [50]. Cell affinity towards synthetic polymers is generally poor as a consequence of their low hydrophilicity and lack of surface cell recognition sites. The incorporation of nano ZrO_2 in synthetic polymer i.e. chitin/chitosan scaffolds were found to have good material characteristics and ideal pore size for tissue engineering and enhanced cell attachment as compared to polymer

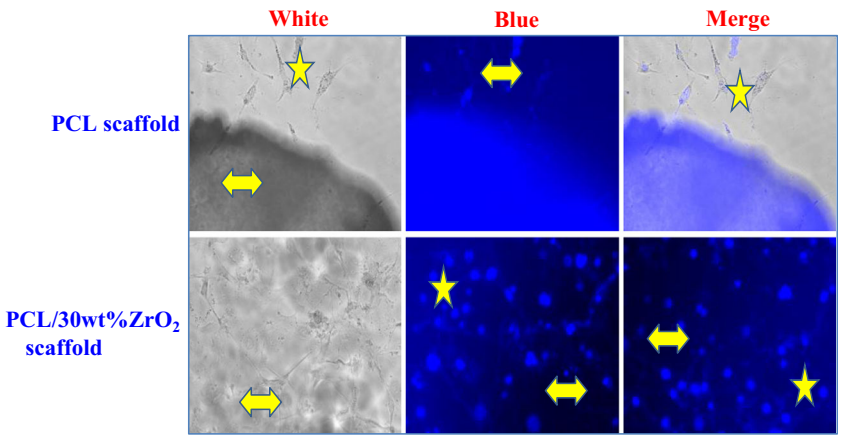

Fig. 8 Fluorescence microscopy images of a culture of mouse fibroblasts 3T3 cells in contact with the PCL and PCL/30wt%ZrO_2 nanofibers scaffold for 5 days (stars indicate fibroblast cells and left-right arrows indicate growth of fibroblast cells on scaffolds surface)

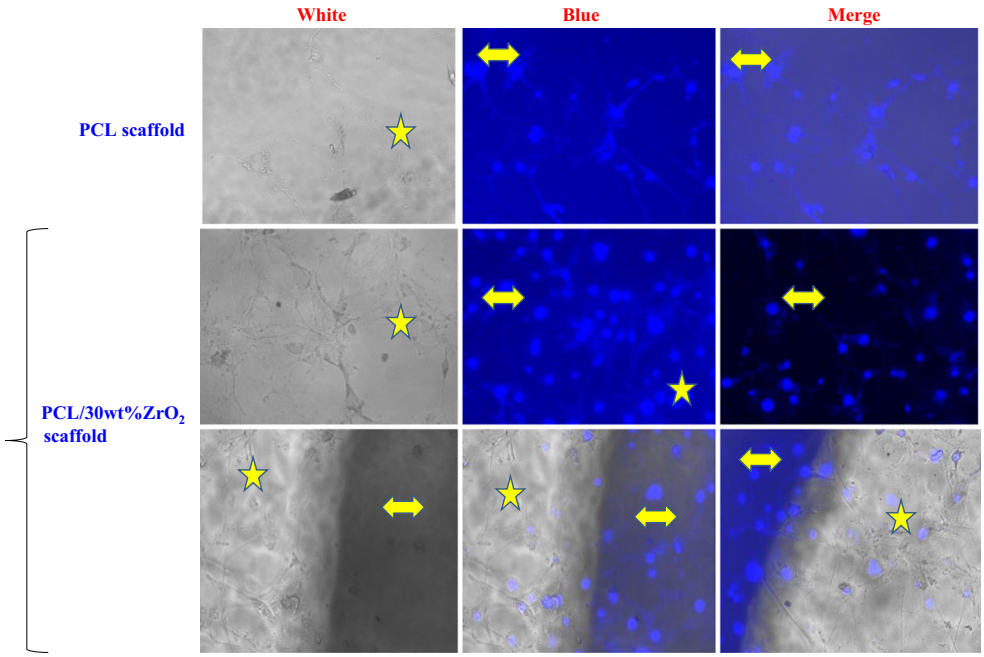

Fig. 9 Fluorescence microscopy images of a culture of mouse fibroblasts 3T3 cells in contact with the PCL and PCL/30wt%ZrO_2 nanofibers scaffold for 7 days (stars indicate fibroblast cells and left-right arrows indicate growth of fibroblast cells on scaffolds surface)

scaffolds [51].Above observation indicated more effectiveness of surface chemistry of PCL/ZrO_2 scaffolds as compared to PCL scaffold to promote proliferation of 3T3 mouse fibroblast cells on these substrates. These results confirmed that PCL/ZrO_2 nanofibers support better cell attachment as compared to the PCL nanofibers due to the addition of Zirconia nanoparticles.

In vitro degradation studies

Degradation of the scaffolds is a very important parameter in tissue engineering. Ideally the scaffolds should degrade as new tissue formation takes place [1]. The in vitro degradation of PCL and PCL/30wt%ZrO_2nanofiber scaffold in PBS was performed for a period of 4 weeks. The PCL scaffold showed increased degradation (51%) as compare to PCL/30wt%ZrO_2scaffolds (49%) (Fig. 10) after 4th week. There is gradual increase in degradation from 1 week to 4 weeks in both scaffolds. Thus the material possesses controlled biodegradation which is suitable for a biomaterial for tissue engineering applications.

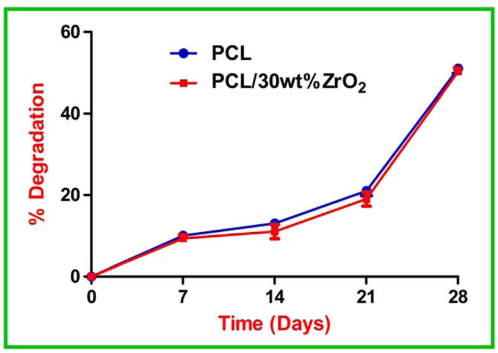

Fig. 10 Degradation of PCL and PCL/30wt%ZrO_2 scaffold

Swelling studies

Swelling facilitates the infiltration of cells into the scaffolds in a three-dimensional fashion, during in vitro cell culture as already proved [52] where desirable swelling and increase in pore size was found to facilitate cell attachment and growth in a three-dimensional fashion. The increase in the pore size also allows cells to avail the maximum internal surface of the scaffolds [53, 54]. Samples showing higher degree of swelling will have a larger surface area/volume ratio thus allowing the samples to have the maximum probability of cell growth in a three-dimensional fashion [55, 56].

The increase in swelling also allows the samples to avail nutrients from culture media more effectively [51]. The mechanical properties of the scaffolds are related to the swelling of the scaffolds. The swelling effect will lose the scaffold from its implanted site and generate unnecessary stress on surrounding tissues. The incorporation of nano ZrO_2 decreased the swelling ability of nano composite scaffolds. This decrease in swelling rate with the addition of nano ZrO_2 may be due to their interaction with PCL and indicating that it had good mechanical strength to support bone tissue in growth. Blending has increased the ability of PCL to absorb water, while retaining its unique characteristics, such as low degradation rate and high mechanical strength [57]. Hence the swelling rate of composite scaffolds (Fig. 11) such as PCL can be controlled by the addition nano ZrO_2.

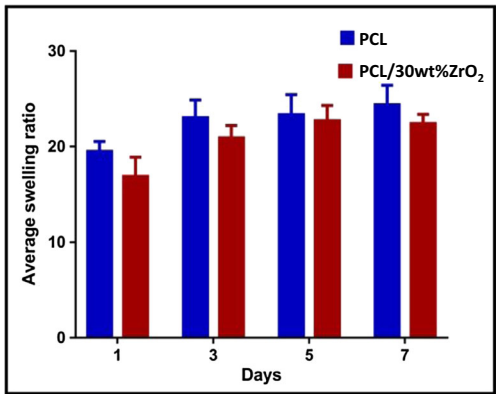

Fig. 11 Swelling data of (**a**) PCL and PCL/30wt%ZrO_2 scaffold

Morphology studies of the nanofibers scaffolds

FE-SEM observations of the cultured 3T3 mouse fibroblast cells in electrospun PCL/30wt%ZrO_2nanofibers scaffolds show some differences in their morphology along the experiment (Fig. 12). At 5 and 7 days of culture, samples from the electrospun PCL nanofiber showed a round-shaped morphology (12(A-B)), In Fig. 12c, referred to the 3T3 cultures at5 days with PCL/30wt%ZrO_2nanofibers scaffolds showed round shape morphology along with the incorporation of ZrO_2 particles on its surface with square shape. At day 7 there was more incorporation of ZrO_2 particles on PCL surface and the shape of particles were round off (Fig. 12d).Our interpretation of these figures is that due to the secretion of ECM components by the 3T3 cells and consequent deposition may lead to a thin film of cells entrapped in this matrix. Therefore, there are less "visible" cells, as they are now part of the matrix. The Same type of study demonstrating the secretion of ECM components by the 3T3 cells was carried out by Silva et al. [58].

Conclusions

Nanofibers scaffolds designed for bone regeneration applications should essentially mimic the vital role of natural tissues. However, the conventional scaffolds lack enough mechanical strength due to higher degradation rate and small surface area for cell growth. Nanofibers composite scaffolds can overcome these limitations. Biodegradable PCL nanofibers composite scaffolds incorporated with biocompatible Zirconia nanoparticles were successfully fabricated by electrospinning of PCL solution. The ZrO_2 was uniformly dispersed on the fiber surfaces for all concentration. These scaffolds were found to have good material characteristics and porosity for tissue regeneration. The scaffold also showed controlled swelling, degradation and enhanced bioactivity in comparison to the control scaffolds. Cell viability studies proved the non-toxic nature of these scaffolds. Finally, the fabricated scaffolds have shown excellent fibroblast cell attachment and proliferation. Thus, this material can be effectively used as tissue-engineering scaffold.

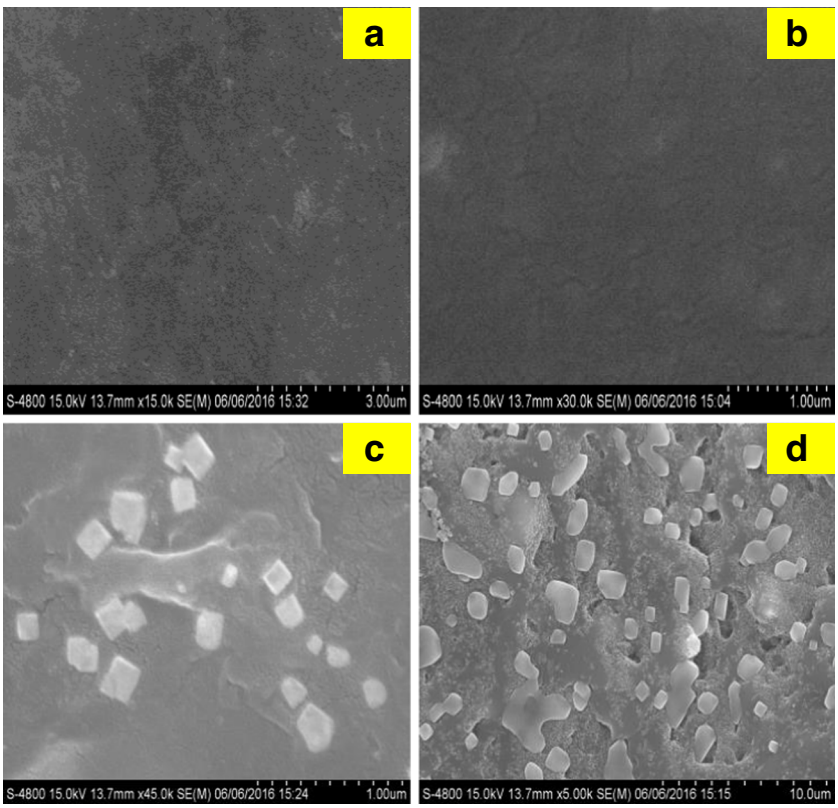

Fig. 12 FE-SEM images of a culture of 3T3 mouse fibroblasts cells in contact with the (**a**- 5 days PCL, **b**- 7 days PCL) and (**c**-5 days PCL/30wt%ZrO_2, **d**-7 days PCL/30wt%ZrO_2) nanofibers scaffold

Acknowledgements Authors are grateful to the University Grant Commission (UGC), New Delhi, for financial support and National Center for Cell Science, Pune for providing cell line.

References

1. Lanza R, Langer R, Vacanti J (2000). Principles of tissue engineering. Academic Press, Elsevier, USA
2. Karp JM, Daltone PD, Shoichet MS (2003). MRS Bull Cell solid 28:301–306
3. Porter JR, Ruckh TT, Popat KC (2009). Biotechnol Prog 25: 1539–1560
4. Hench LL, Polak JM (2002). Science 295:1014–1017
5. Brown TD, Fredrik EN, Anthony DS, Dietmar WH, Paul DD (2014). Mater Sci Eng C 45:698–708
6. Kmita AR, Slosarczyk A, Paszkiewicz Z, Paluszkiewicz C (2004). J Mol Struct 704:333–340
7. Temenoff JS, Mikos AG (2000). Injectable biodegradable materials for orthopedic tissue engineering. Biomaterials 21:2405–2412
8. Gupta KC, Haider A, Choi Y, Kang I (2014). Biomater Res 18:1–11
9. Hagvall SH, Schenke LK, Dhanasopon AP, Rofail F, Smith H, Wu BM (2008). Biomaterials 29:2907–2914
10. Zhang X, Reagan MR, Kaplan DL (2009). Adv Drug Deliv Rev 61: 988–1006
11. Murugan R, Ramakrishna S (2007). Design strategies of tissue engineering scaffolds with controlled fiber orientation. Tissue Eng 13: 1845–1866
12. Obrien FJ (2011). Biomaterials and scaffolds for tissue engineering. Mater Today 14:88–95
13. Yunos DM, Bretcanu O, Boccaccini AR (2008). J Mater Sci 43: 4433–4442
14. Kumber SG, James R, Nukavarapu SP, Laurencin CT (2008) Electrospun nanofiber scaffolds: engineering soft tissues. Biomed Mater. https://doi.org/10.1088/1748-6041/3/3/034002
15. Alhosseini SN (2012). Int J Nanomedicine 7:25–34
16. Wang X, Ding B, Li B (2013). Mater Today 16:229–241
17. Hasan M, Nayem KA, Hossain MB, Nahar S (2014). Int J Textile Sci 3:39–43
18. Detta N (2010). Polym Int 59:1558–1562
19. Kanani AG, Bahrami SH (2010). Trends Biomater Artif Organs 24: 93–105
20. Srinivas M, Buvaneswari G (2006). Trends Biomater Artif Organs 20:24–30
21. Thakare VG, Joshi PA, Godse RR, Bhatkar VB, Wadegaokar PA, Omanwar SK (2016). Int J Pharm Pharm Sci 8:125–131
22. Ramires PA, Romito A, Cosentino F, Milella E (2001). Biomaterials 22:1467–1474
23. Zhensheng L, Ramay HR, Hauch KD, Xiao D, Zhang M (2006). Biomaterials 26:3919–3928
24. Amy C, Daniel H, Wang R (2006). Biomaterials 34:2343–2350
25. Roualdes O, Duclos ME, Gutknecht D, Frappart L, Chevalier J, Hartmann DJ (2010). Biomaterials 31:2043–2054
26. Oetzel C, Clase ER (2006). J Mater Sci 41:8130–8137
27. Thakare VG (2012). Int J Eng Res Dev 5:25–28
28. Wang L, Shelton RM, Cooper PR, Lawson M, Triffitt JT, Barralet JE (2003). Biomaterials 24:3475–3481
29. Majeti NVR (2000). React Funct Polym 46:1–27
30. Pilathadka S, Vahalova D, Vosahlo T (2007). Prague Med Rep 108: 5–12
31. Stefanic M, Krnel K, Kosmac T (2010). Biomaterials 31: 2043–2054
32. Hedaoo VP, Bhatkar VB, Omanwar SK (2015). Opt Mater 45: 91–96
33. Khan ZS, Ingale NB, Omanwar SK (2015). Mater Lett 2: 4384–4389
34. Mohamed G (2012). J Ind Tex 41:222–240
35. Chatzistavrou X, Fenno JC, Faulk D, Badylak S, Kasuga T, Boccaccini AR (2014). Acta Biomater 10:3723–3732
36. Trusova EA, Khrushcheva AA, Vokhmintcev KV (2012). J Eur Ceram Soc 32:1977–1981
37. Kim JS, Lee DH, Kang S, Bae DS, Paek HY, Na MK (2009). Trans Nonferrous 19:88–91
38. Scherrer P (1918). Math-Phys Klasse 2:98–100
39. Langford J, Wilson A (1978). J Appl Crystallogr 11:102–113
40. Lao L, Wang Y, Zhu Y, Zhang Y, Gao C (2011). J Mater Sci Mater Med 22:1873–1884
41. Augustine R, Malik HN, Singhal DK, Mukherjee A, Malakar D, Kalarikkal N, Thomas S (2014). J Polym Res 21:347–363
42. Radev L, Vladov D, Michailova I, Cholakova E, Fernandes MFV, Salvado IIM (2013). Int J Mater Chem 3:91–98
43. Thakare VG, Joshi PA, Godse RR, Bhatkar VB, Wadegaokar PA, Omanwar SK (2016) Trends biomate. Artif Organs 30:126–133
44. Jothi S, Prithivikumaran N, Jeyakumaran N (2014). Int J ChemTech Res 6:1971–1973
45. Vasita R, Katti DS (2006). Int J Nanomedicine 1:15–30
46. Jayakumara R (2011). Int Bio Macromol 49:274–280
47. Zhang YZ, Su B, Venugopal J, Ramakrishna S, Lim CT (2007). Int J Nanomedicine 2:623–638
48. Zhao L, He C, Gao Y, Cen L, Cui L, Cao Y (2008). J Biomed Mater Res 87:8726–8734
49. Brien FJO (2014). Mater Today 14:141–148
50. Mobarakeh LG, Prabharan MP, Tian L, Jeshvadhani ES, Dehghani L, Dehghani L, Ramakrishna (2015). World J Stem Cells 7:728–744
51. Jayakumara R (2011). Int J Biol Macromol 49:274–280
52. Shanmugasundaram N, Ravichandran P, Reddy PN, Ramamurty N, Pal S, Rao KP (2001). Biomaterials 22:1943–1951
53. Langer R, Vacanti JP (1993). Science 260:920–926
54. Mikos AG, Sarakinos G, Lyman MD, Vacanti DE, Langer R (1993). Biotechnol Bioeng 42:716–723
55. Vacanti JP, Langer R (1999). Lancet 354:32–34
56. Blaker JJ, Gough JE, Maquet V, Notingher I, Boccaccini AR (2003). J Biomed Res A 67:1401–1411
57. R. M. Jin, N. Sultana, S. Baba, S. Hamdan, A. F. Ismail, J Nanomate (2015) Article ID 357372
58. Silva MLA, Martins A, Pinto AR, Costa P, Faria S, Gomes M, Reis RL, Neves NM (2010). Cartilage tissue engineering using electrospun PCL nanofiber meshes and MSCs. Biomacromolecules 11:3228–3236